# Model-Based Segmentation of Hippocampal Subfields in Ultra-High Resolution In Vivo MRI

Koen Van Leemput[1,2], Akram Bakkour[1,3], Thomas Benner[1], Graham Wiggins[1], Lawrence L. Wald[1,4], Jean Augustinack[1], Bradford C. Dickerson[1,3], Polina Golland[2], and Bruce Fischl[1,2,4]

[1] *Athinoula A. Martinos Center for Biomedical Imaging, Department of Radiology, MGH, Harvard Medical School, USA*
[2] *Computer Science and Artificial Intelligence Laboratory, MIT, USA*
[3] *Department of Neurology, MGH, Harvard Medical School, USA*
[4] *Harvard-MIT Division of Health Sciences and Technology, MIT, USA*

MGH/HST Athinoula A. Martinos Center for Biomedical Imaging

MASSACHUSETTS GENERAL HOSPITAL

HST Harvard-MIT Health Sciences & Technology

CSAIL

MIT COMPUTER SCIENCE AND ARTIFICIAL INTELLIGENCE LABORATORY

http://picsl.upenn.edu/caph08/papers/paper04.pdf

# Motivation

✓The hippocampus consists of multiple, interacting subregions *(cf. talk by Susanne Mueller)*

✓Distinct hippocampal subregions:

- are implicated in different memory subsystems
- are differentially affected in different conditions and disease processes (normal aging, Alzheimer's disease (AD), …)

⇨ The ability to measure these subregions using *in vivo* neuroimaging is of great potential value:

Basic neuroscience: *insights into the function and structure of the hippocampus in the living human brain, and how it is affected in normal aging.*

Clinical research: *sensitive, non-invasive biomarkers for early diagnosis and treatment evaluation in AD. Surrogate outcome markers in clinical treatment trials.*

# Motivation

✓ Recent developments in MR data acquisition technology are starting to yield images that show anatomical features of the hippocampal formation at an unprecedented level of detail

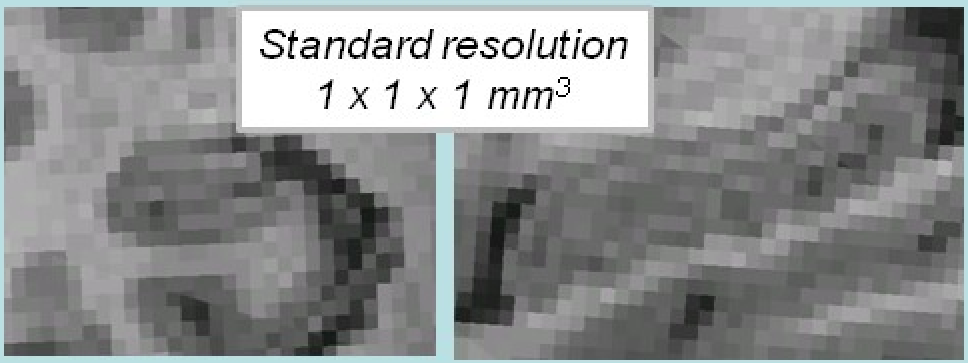


New opportunities for explicitly quantifying individual subregions, rather than their agglomerate, directly from *in vivo* MRI

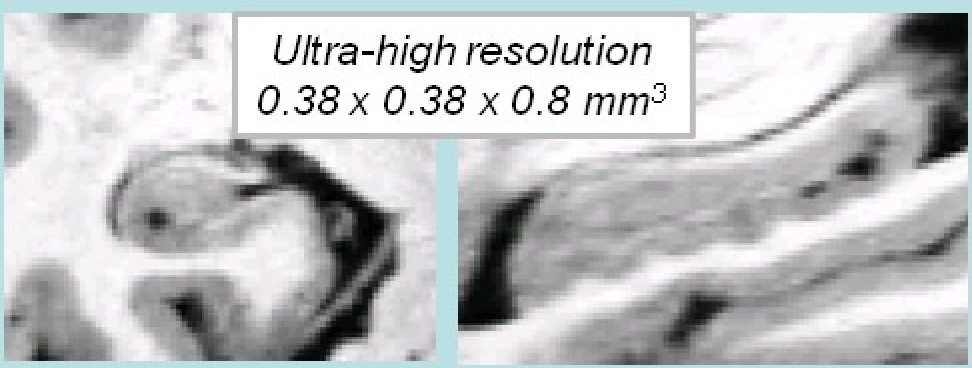


Analyzing large imaging studies of ultra-high resolution MRI scans requires **automated computational techniques**

# Model-based segmentation

- ✓ Derive computational models from manual delinations in a number of subjects
- ✓ Use those models to automatically segment MRI scans of new subjects

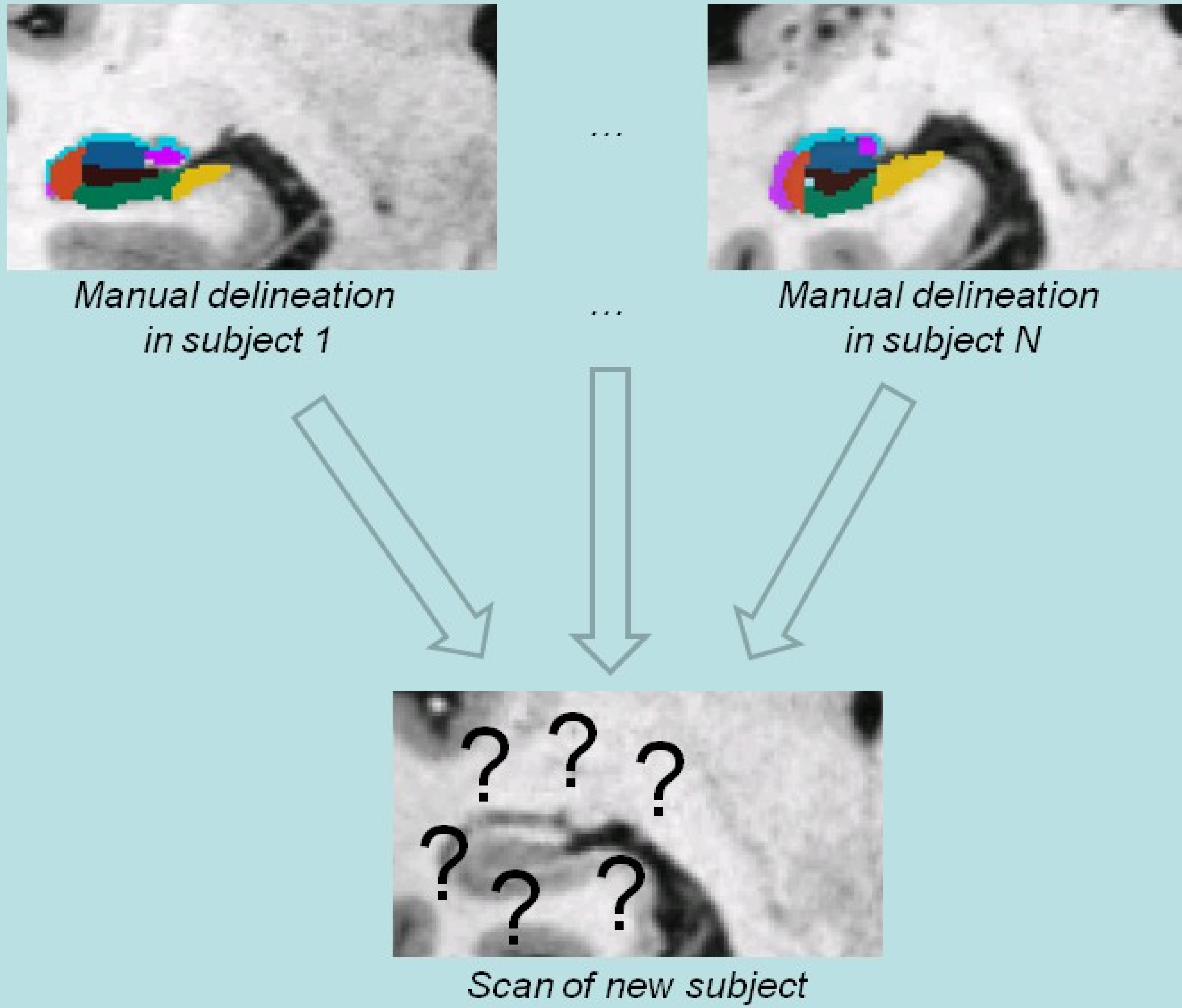

# Bayesian modeling

"labeling model"

$$p(\boldsymbol{L}|\Phi_L)$$

$$p(\Phi_L)$$

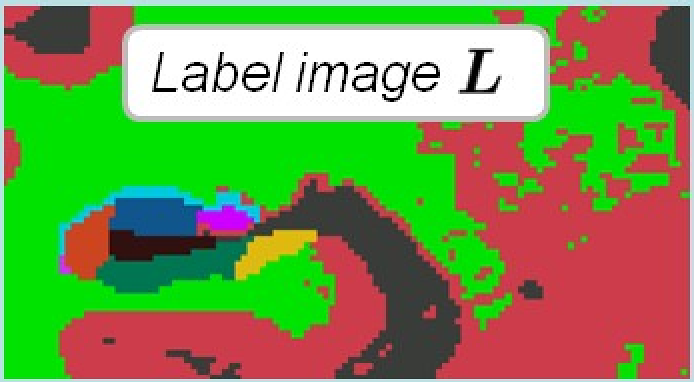


"imaging model"

$$p(\boldsymbol{Y}|\boldsymbol{L}, \Phi_Y)$$

$$p(\Phi_Y)$$


**_Step 1_**

✓ Invent a generative model of image formation
  - A mathematical model of how an MRI image is formed
  - Depends on some model parameters

$$\Phi = \{\Phi_Y, \Phi_L\}$$

# Bayesian modeling

"labeling model" $p(\boldsymbol{L}|\Phi_L)$ $p(\Phi_L)$

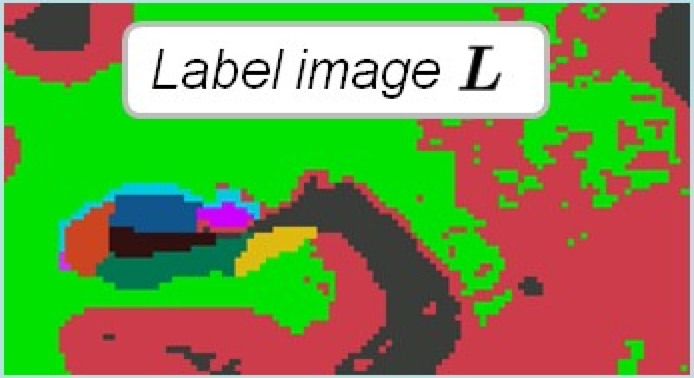


"imaging model" $p(\boldsymbol{Y}|\boldsymbol{L},\Phi_Y)$ $p(\Phi_Y)$


**_Step 2_**

✓ Use the generative model to obtain the most probable segmentation given an MRI image

$$\begin{aligned}\widehat{\boldsymbol{L}} &= \arg\max_{\boldsymbol{L}} p(\boldsymbol{L}|\boldsymbol{Y}) \\ &= \arg\max_{\boldsymbol{L}} \int_{\Phi} p(\boldsymbol{L}|\boldsymbol{Y},\Phi)p(\Phi|\boldsymbol{Y})\mathrm{d}\Phi \\ &\simeq \arg\max_{\boldsymbol{L}} p(\boldsymbol{L}|\boldsymbol{Y},\widehat{\Phi})\end{aligned}$$

✓ Involves **_two_** optimizations:

- First estimate the optimal model parameters $\widehat{\Phi}$
- Then find the optimal segmentation based on those parameter estimates

# Labeling model

"labeling model" $p(\boldsymbol{L}|\Phi_L)$

$p(\Phi_L)$

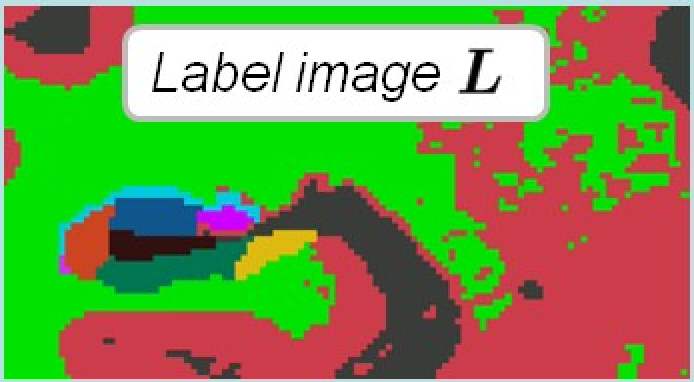


"imaging model" $p(\boldsymbol{Y}|\boldsymbol{L}, \Phi_Y)$

$p(\Phi_Y)$

# Labeling model

"labeling model"

$p(\boldsymbol{L}|\Phi_L)$

$p(\Phi_L)$

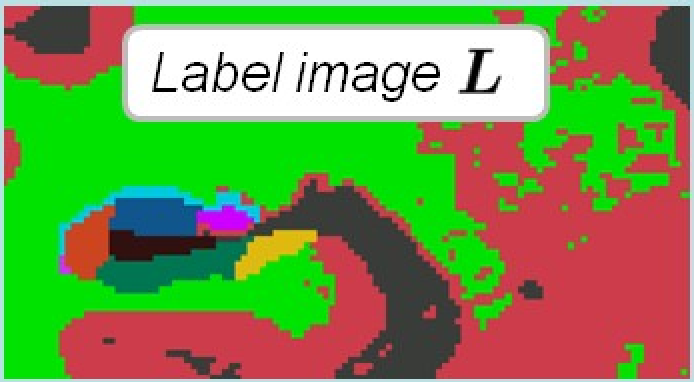


"imaging model"

$p(\boldsymbol{Y}|\boldsymbol{L},\Phi_Y)$

$p(\Phi_Y)$


✓The label image is modeled as being generated by deforming a probabilistic atlas, and sampling the voxel labels from the deformed atlas

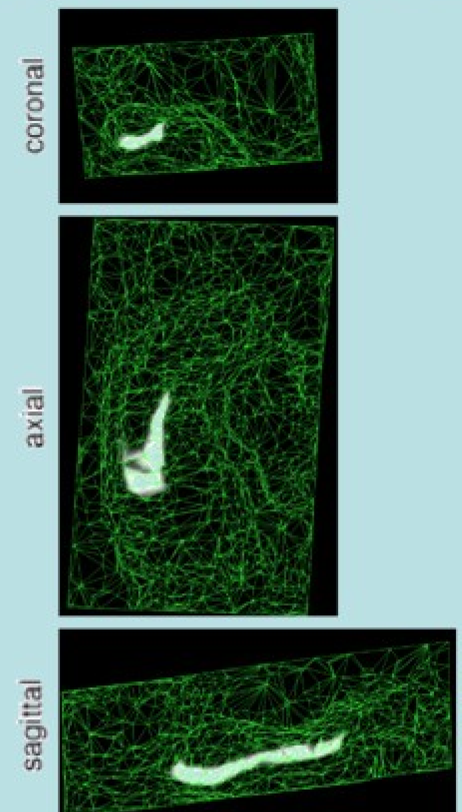


*Prior probability for subiculum*

- Tetrahedral mesh atlas representation
- The parameters $\Phi_L$ are the location of the mesh nodes
- The prior $p(\Phi_L)$ penalizes deformations and is topology-preserving *[Ashburner et al., 2000]*

# Labeling model

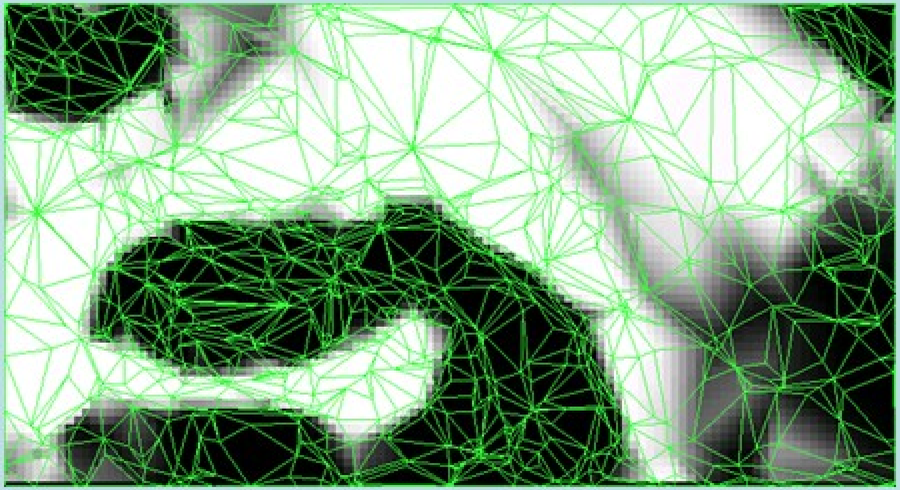

*probability for white matter*

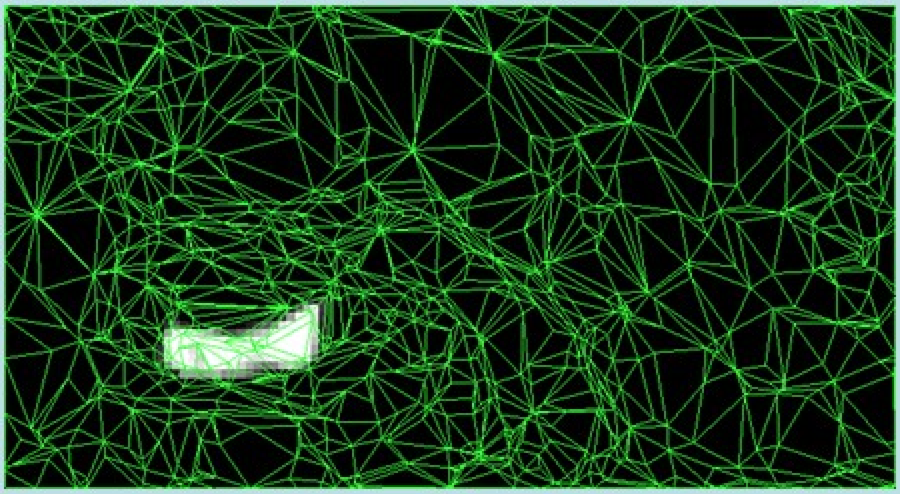

*probability for subiculum*

*… etc …*

# Labeling model

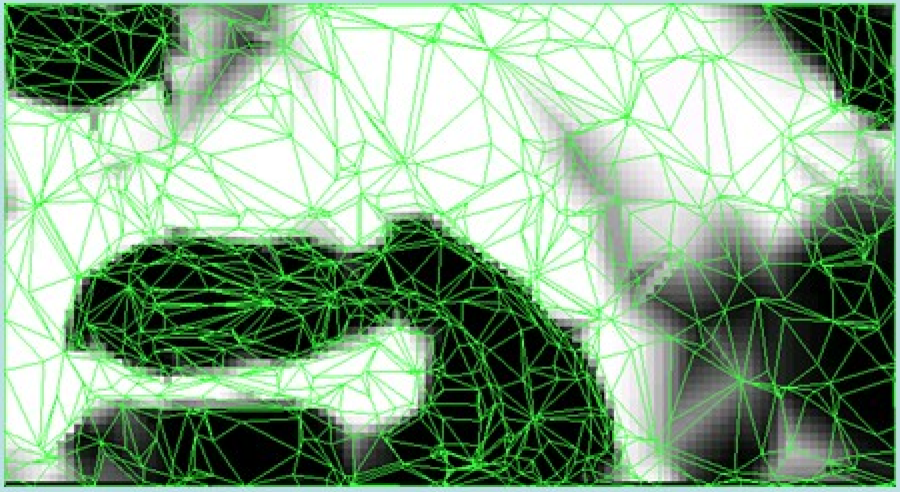

*deformed probability for white matter*

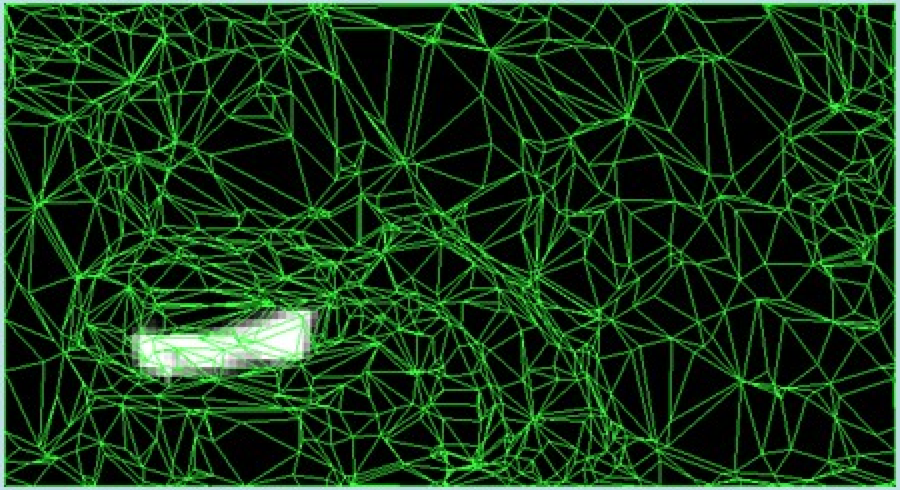

*deformed probability for subiculum*

*… etc …*

# Labeling model

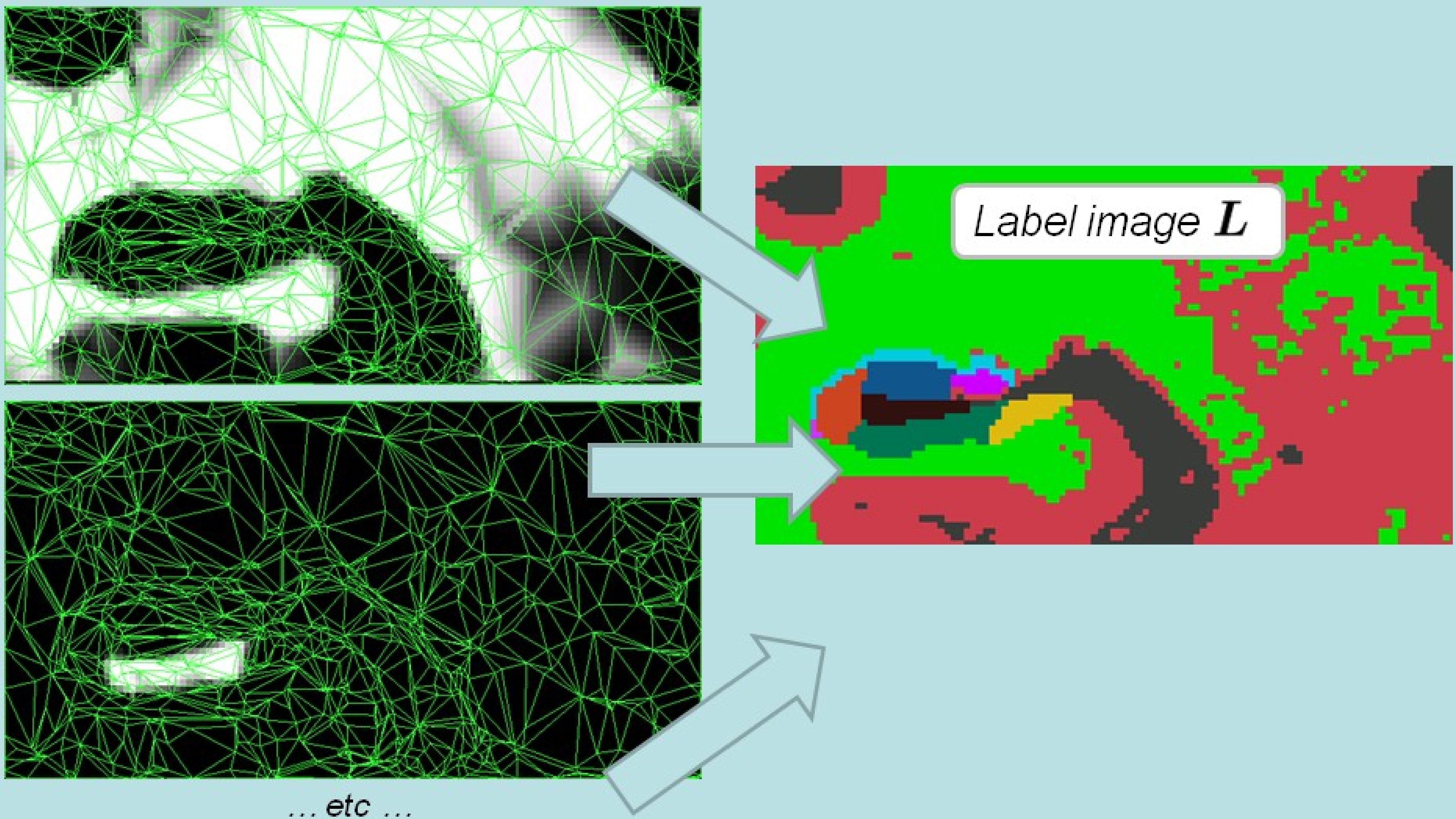

# So where does the atlas come from?

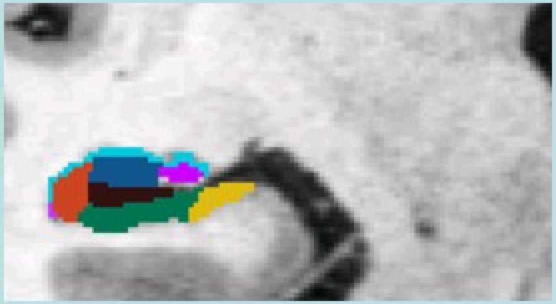

…

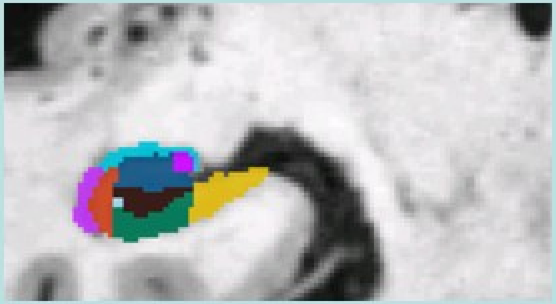

*Manual delineation in subject 1* … *Manual delineation in subject N*

- ✓ Manual delineations in N subjects are "augmented" with automated tissue classification in non-labeled voxels
- ✓ The resulting label images are modeled as being generated by the deformable mesh-based labeling model described before
- ✓ Bayesian inference: *[Van Leemput, MICCAI 2006], [Van Leemput, TMI 2008 (submitted)]*
  - For a given mesh representation, what are the most likely label probabilities in the mesh nodes? ⇨ Group-wise registration
  - What is the most likely mesh representation?

⇨
- Automatically penalizes overly complex models (cf. MDL)
- Compact mesh representations
- Avoids overfitting to the training data

# Imaging model

"labeling model" $p(\boldsymbol{L}|\Phi_L)$ $p(\Phi_L)$


"imaging model" $p(\boldsymbol{Y}|\boldsymbol{L}, \Phi_Y)$ $p(\Phi_Y)$

# Imaging model

"labeling model" $p(\boldsymbol{L}|\Phi_L)$ $p(\Phi_L)$


"imaging model" $p(\boldsymbol{Y}|\boldsymbol{L}, \Phi_Y)$ $p(\Phi_Y)$


✓The intensity in each voxel is modeled as being drawn independently from a Gaussian distribution associated with its label

- The model parameters $\Phi_Y$ are the means and variances of the Gaussians
- We assume a uniform prior $p(\Phi_Y)$

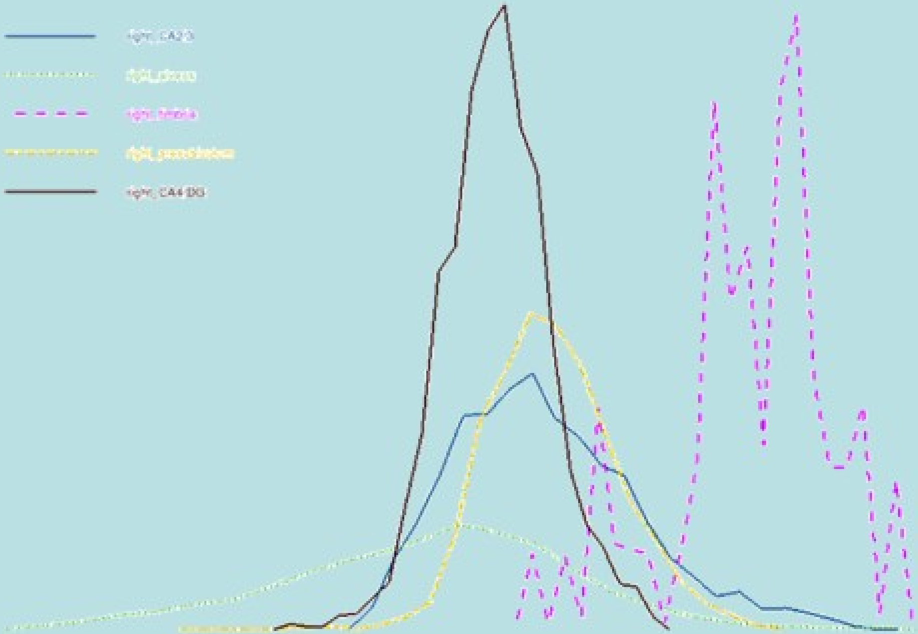

# Model parameter optimization

- ✓ Given an MR image $\boldsymbol{Y}$ that is to be segmented, what are the most probable model parameters $\Phi = \{\Phi_Y, \Phi_L\}$?
  - $\Phi_Y$: *Mean and variance of the Gaussian distribution associated with each neuroanatomical label*
  - $\Phi_L$: *Position of the nodes of the mesh (atlas warp)*
- ✓ Parameter optimization performed with a Generalized Expectation Maximization algorithm

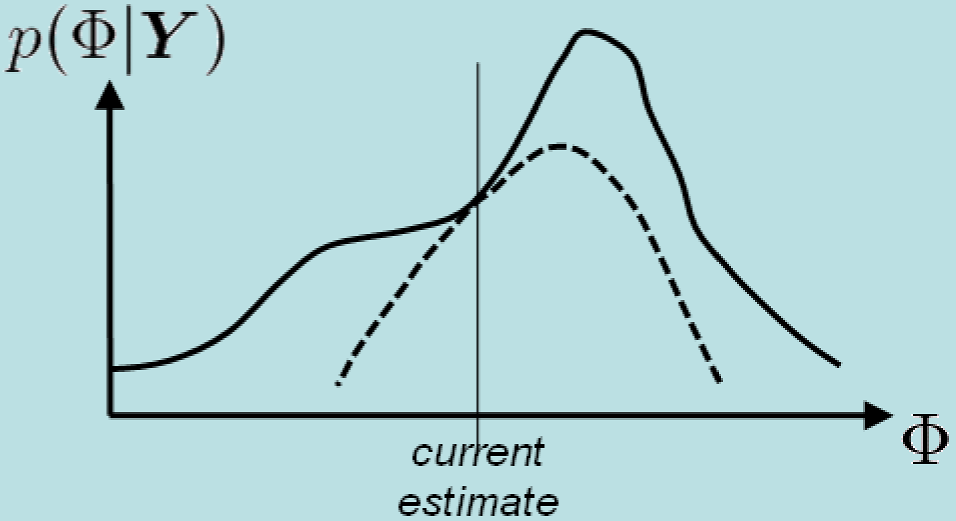


- Repeatedly try to improve a lower bound to the objective function
- Each improvement automatically means an improvement in the objective function

# Model parameter optimization

✓ Improve lower bound w.r.t. the atlas warp, keeping the Gaussian distribution parameters fixed at their current values

- Calculate a statistical classification
- Warp the atlas onto this classification (cf. *[D'Agostino 2006, Pohl 2006])*
- Gradient descent

✓ Improve lower bound w.r.t. the Gaussian distribution parameters, keeping the altas warp fixed at its current value

- Calculate a statistical classification
- Closed-form expressions for Gaussian distribution parameters

Statistical classification of each voxel depends on how well its intensity is explained by each label's Gaussian distribution **and** by the prior probability for each label in the atlas in its current deformation

# Model parameter optimization

✓ Improve lower bound w.r.t. the atlas warp, keeping the Gaussian distribution parameters fixed at their current values

- Calculate a statistical classification
- Warp the atlas onto this classification (cf. *[D'Agostino 2006, Pohl 2006]*)
- Gradient descent

✓ Improve lower bound w.r.t. the Gaussian distribution parameters, keeping the altas warp fixed at its current value

- Calculate a statistical classification
- Closed-form expressions for Gaussian distribution parameters

Statistical classification of each voxel depends on how well its intensity is explained by each label's Gaussian distribution **and** by the prior probability for each label in the atlas in its current deformation

Upon converge of the parameter estimation algorithm, the optimal labeling $\widehat{L}$ is obtained by assigning each voxel to the most probable label

# Experiments

- ✓ Ultra-high resolution (0.38 x 0.38 x 0.8 $mm^3$) MRI data
  - 3T Siemens Trio with prototype custom-built 32-channel coil
  - Optimized MPRAGE sequence, 208 coronal slices
  - 5 acquisitions; motion-corrected and resampled to 0.38mm isotropic

- ✓ Manual segmentation of the right hippocampus in 5 subjects (2 young + 3 older cognitive normal)
  - Fimbria, CA1, CA2/3, CA4/DG, presubiculum, subiculum, hippocampal fissure + surrounding structures
  - Extremely time consuming: 1 -> 2 weeks ***per hippocampus***!

Validation of the automated segmentation algorithm using leave-one-out cross-validation

# Qualitative results

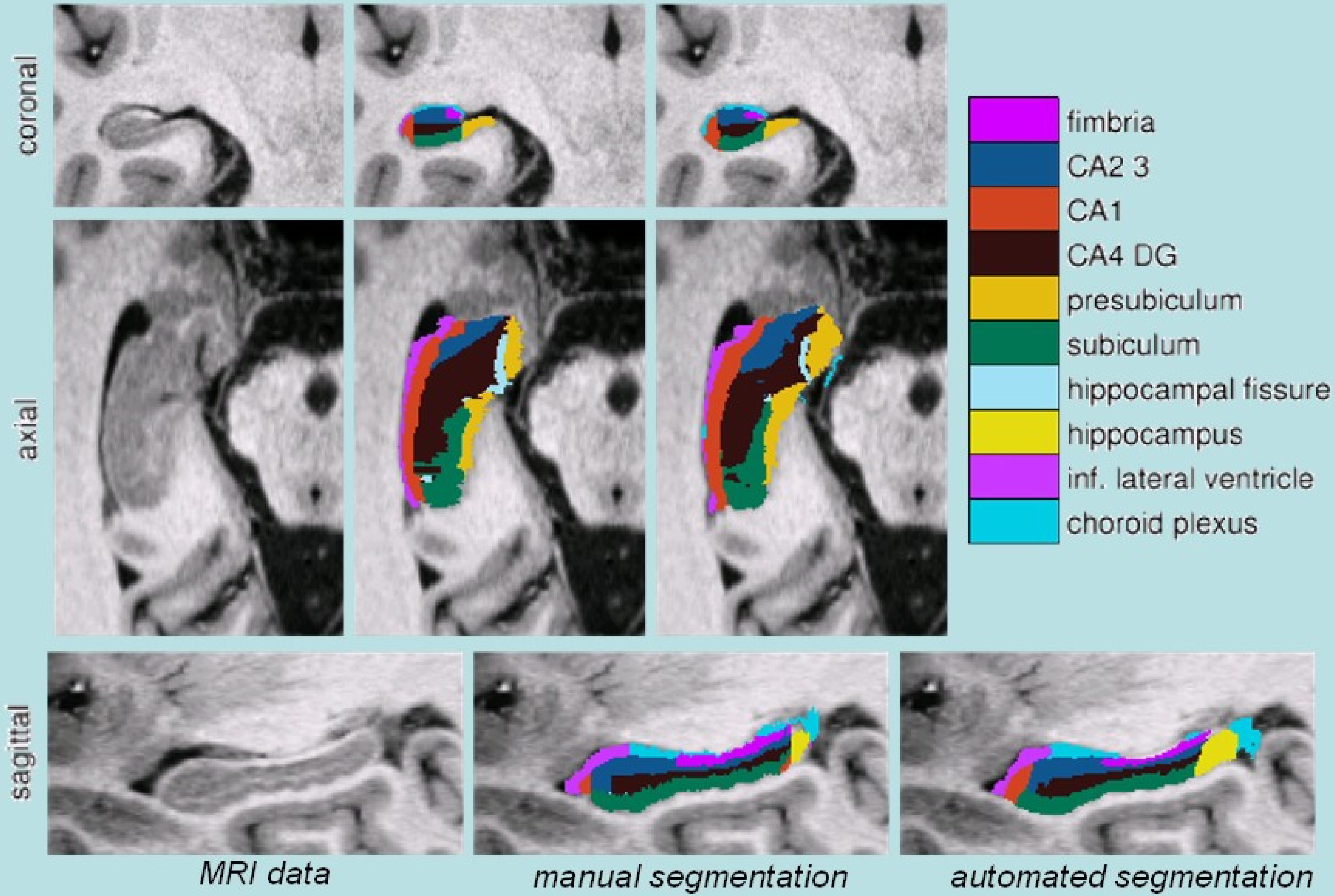

# Qualitative results

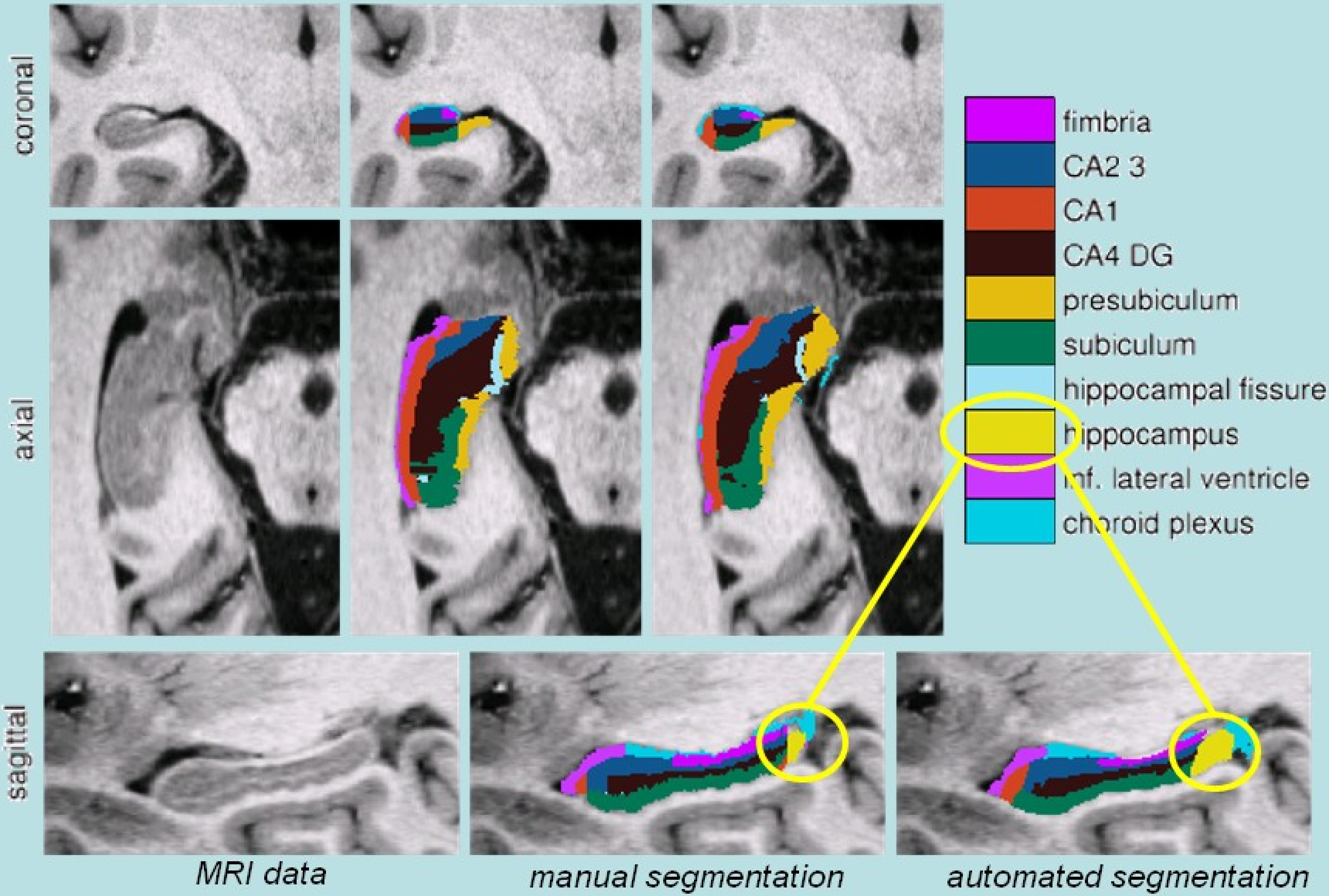

# Quantitative results: spatial overlap

- ✓Dice coefficient for automated vs. manual segmentation
  - ( volume of overlap ) / ( average volume )
- ✓Excluded the "catch-all" label towards the tail of the hippocampus

# Quantitative results: volume measurements

✓Volume differences between manual vs. automated segmentations

✓Linear regression between volume measurements with both methods (Pearson's correlation coefficient)

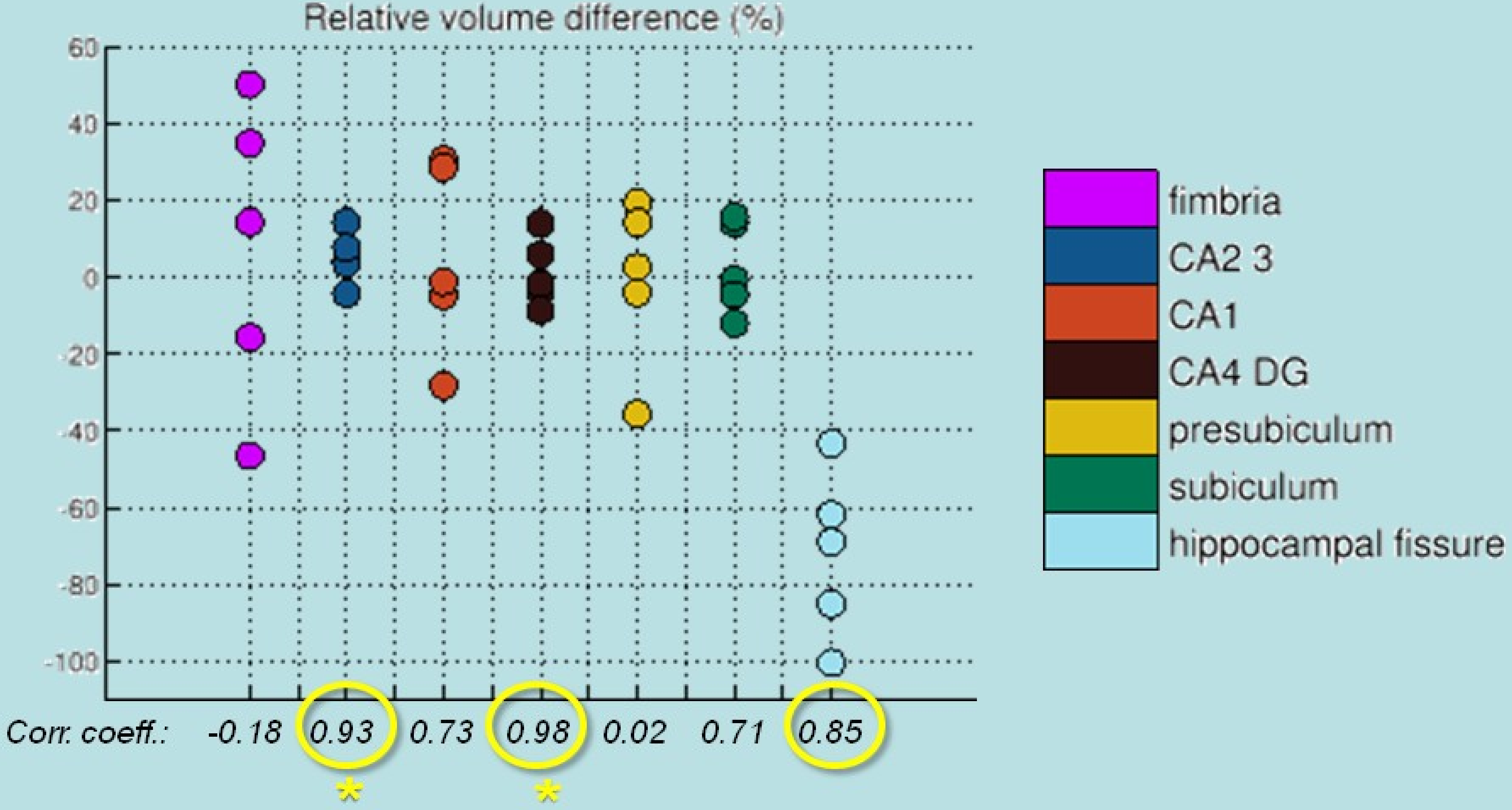

# Future (current) work

✓ More thorough validation

– Repeated manual labelings of the same subjects

– Human intra- and inter-rater variability provides context for validation

✓ Modified imaging model to take partial volume effect into account

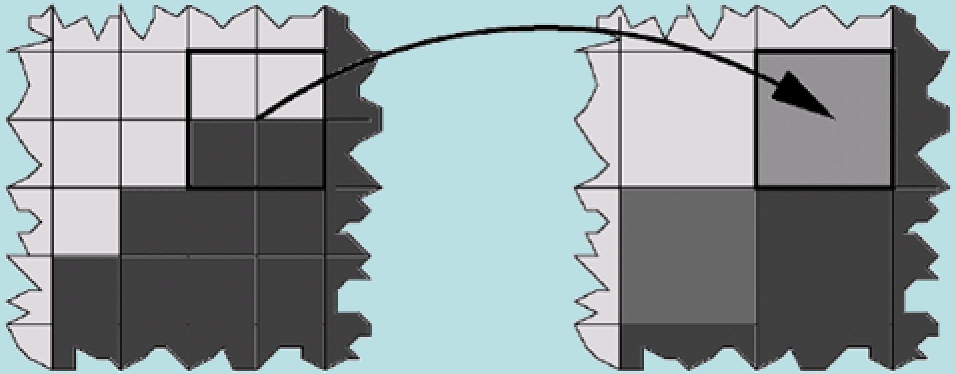

*[Van Leemput, TMI 2003]*

– Segment hippocampal subfields in standard resolution ($1 \times 1 \times 1$ $mm^3$) scans

– Alzheimer's Disease Neuroimaging Initiative (ADNI)

– Open Access Series of Imaging Studies (OASIS) project

– Hopefully with a reasonable reliability ☺

# Acknowledgements

✓ *Support for this research was provided in part by:*

- *the NIH NCRR (P41-RR14075, R01 RR16594-01A1, NAC P41-RR13218, and the BIRN Morphometric Project BIRN002, U24 RR021382)*
- *the NIBIB (R01 EB001550, R01EB006758, NAMIC U54-EB005149)*
- *the NINDS (R01 NS052585-01, R01 NS051826)*
- *the MIND Institute.*
- *The Autism & Dyslexia Project funded by the Ellison Medical Foundation*